Optical edge projection for surface contouring

Wu, X. P.; Miao, Hong; Quan, Chenggen; Tay, Cho Jui; Fu, Yu

2005

Miao, H., Quan, C., Tay, C. J., Fu, Y., & Wu, X. P. (2005). Optical edge projection for surface contouring. Optics Communications.

https://hdl.handle.net/10356/92122

https://doi.org/10.1016/j.optcom.2005.06.029

Optical edge projection for surface contouring

H. Miao [a,b], C. Quan [a,*], C.J. Tay [a], Y. Fu [a], X.P. Wu [b]

[a] Department of Mechanical Engineering, National University of Singapore, 10 Kent Ridge Crescent, Singapore 119260, Singapore
[b] Key Laboratory of Mechanical Behavior and Design of Materials, Department of Modern Mechanics, University of Science and Technology of China, Hefei, Anhui 230027, China

[*]Corresponding author. Tel.: +65 6874 8089; fax: +65 6779 1459.
E-mail address: mpeqcg@nus.edu.sg (C. Quan).

Abstract

A novel optical edge projection method is proposed for surface contouring of an object with low reflectivity. A structured light edge is projected onto a dark surface, and the image is captured by a CCD camera. The object contour is evaluated using active triangular projection algorithm, and a whole field 3D contour of the object is obtained by scanning the optical edge over the entire object surface. The proposed method is applied to a black low-reflective object made of weaved carbon fiber. The results which are verified with conventional phase shifting fringe projection technique show that an accurate profile of a specimen can be obtained. The proposed method is also applied to surface contouring of a small component.

Keywords: Fringe projection; Optical edge; Surface contouring

1. Introduction

Optical techniques are widely used to determine surface contour in many engineering fields. Generally they are non-contact and non-destructive, and are desirable for vibration analysis, quality control and contour mapping. Common optical methods for contouring include moiré [1,2], holography [3], Fourier transform [4,5], phase measuring profilometry [6,7], and shearography [8,9]. In recent years, phase shifting fringe projection method [10,11] has become a predominant method for surface contouring, and has been extended to measurement of micro components.

When a structured light is projected onto the surface of an object, the projected fringe pattern is perturbed due to its profile, thereby enabling direct derivation of the surface profiles. Conventional phase shifting fringe projection method produces good results when the surface of the object has good reflectivity. However, if the surface has low reflectivity, such as a weaved carbon fiber, large error will result due to low image intensity.

To overcome this problem, a novel optical edge projection method is proposed. A structured light edge is projected onto an object and the distorted optical edge is captured by a CCD camera. Extracting the optical edge shadow and comparing it with a reference

line, the height of the object surface along the edge can be obtained using the triangulation method. Whole field 3D contour of the object is obtained by scanning the optical edge over the entire object surface. The accuracy of the method is dependent upon that of the optical edge detection algorithm. In this paper, the Canny edge detector [12] designed specially for step edge extraction [13] is used.

2. Principle of the method

2.1. Active triangulation projection

Fig. 1 shows a schematic of the projection and imaging system. It is an active triangulation projection semi-whole-field measuring system. An optical edge is projected onto a specimen at right angle. The image of the edge is located along point *A* and *O* is the corresponding point on a reference line. When viewed from another direction at an angle θ, a distorted image *AC* can be observed. The height $h(x,y)$ of point *A* can be calculated directly from simple geometry.

As shown in Fig. 1, the height of the specimen surface $h(x,y)$ can be obtained by

$$h(x,y) = AC/\sin\theta, \tag{1}$$

AC indicates the projected optical edge; the length of *AC* which is calculated from the reference line is in units of pixels. The actual values of *AC* are calculated from a calibrated reference line.

2.2. Optical edge detection

In Canny edge detection algorithm [12], a two-dimensional Gaussian function $G(x,y)$ is given by:

$$G(x,y) = \frac{1}{2\pi\sigma^2}\exp\left(-\frac{x^2+y^2}{2\sigma^2}\right) \tag{2}$$

and an image with an optical edge $f(x,y)$ is smoothened by convolution with $G(x,y)$. The smoothened image $G[f(x,y)]$ is

$$G[f(x,y)] = G(x,y) * f(x,y). \tag{3}$$

Two-dimensional first derivatives are then calculated, and the gradient magnitude (edge strength) and direction are obtained. The first-order derivative of an image $f(x,y)$ at a point $P(x,y)$ is defined by a two-dimensional vector

$$G[f(x,y)] = \begin{bmatrix} Gf_x \\ Gf_y \end{bmatrix} = \begin{bmatrix} \frac{\partial Gf}{\partial x} \\ \frac{\partial Gf}{\partial y} \end{bmatrix}. \tag{4}$$

The absolute gradient magnitude is given by:

$$|G[f(x,y)]| = |G_x^2 + G_y^2|^{1/2}. \tag{5}$$

The gradient direction (edge orientation) is defined by:

$$\theta = \arctan\frac{G_y}{G_x} - \frac{3}{4}\pi. \tag{6}$$

A non-maximal suppression process is then applied to the gradient magnitude (edge strength) image to identify the local maxima. Only pixels with edge strength larger than their two adjacent pixels in the gradient direction are identified as edge candidates while the others are set to zero. The non-maximal suppression process results in edge segments of one pixel width. To remove false edge segments due to noise, a thresholding with hysteresis is processed. Two thresholds estimated by a signal-to-noise ratio from the original image are used to remove weak edges using the following criteria: (1) all edge candidates below the lower threshold value are marked as background; (2) edge candidates above the lower threshold are identified as edge pixels if they can be connected to any pixels above the high threshold through a chain of edge pixels.

2.3. Surface contouring by phase shifting technique

The phase shifting fringe projection technique is also used for comparison. Four phase shifted sinusoidal fringes with phase shifts of 0, $\pi/2$, π and $3\pi/2$ are projected onto a test surface. The following equations represent the four successive intensity distributions [14]:

$$I_1(x,y) = a(x,y) + b(x,y)\cos\varphi(x,y), \tag{7}$$

$$I_2(x,y) = a(x,y) + b(x,y)\cos[\varphi(x,y) + \pi/2], \tag{8}$$

$$I_3(x,y) = a(x,y) + b(x,y)\cos[\varphi(x,y) + \pi], \tag{9}$$

$$I_4(x,y) = a(x,y) + b(x,y)\cos[\varphi(x,y) + 3\pi/2], \tag{10}$$

where $a(x,y)$ is an average intensity (background), $b(x,y)$ is the intensity modulation, and $\varphi(x,y)$ are the phase values to be determined. The phase $\varphi(x, y)$ at each point on the image can be obtained by

$$\varphi(x,y) = \arctan\frac{I_4(x,y) - I_2(x,y)}{I_1(x,y) - I_3(x,y)}. \tag{11}$$

The calculated phase $\varphi(x, y)$ are principal values in the range of $(-\pi, \pi)$, and is wrapped in this range with discontinuous 2π phase jumps if the variation is larger than 2π. The discontinuity can be removed by the phase unwrapping process [15,16] and the object height $h(x,y)$ is obtained from the unwrapped phase map using [11]

$$h(x,y) = k\varphi(x,y), \tag{12}$$

where *k* is an optical coefficient related to the configuration of the system.

3. Experimental work

Two test specimens are used in this study. The first specimen consists of a flat plate fabricated with weaved carbon fiber material. Fig. 2 shows an optical edge projection on the specimen. The surface has a very low reflectivity and is highly uneven due to its weaved structure. Numerous valleys can be observed between the fibers. To view these valleys, a powerful white light source is needed. The optical edge is projected by a 150 W DC white light source at a right angle using optical fiber through a set of imaging lenses onto an area of 25 mm x 15 mm. The distorted optical edge is captured by a CCD camera mounted at an angle to the light source. In phase shifting fringe projection, the optical arrangement used is similar to that shown in Fig. 1. The edge projection in this case is replaced with a liquid crystal display (LCD) projector controlled by a computer. The phase shifted fringes are subsequently captured with the CCD camera and phase maps are subsequently obtained.

Fig. 3 shows a second specimen indicating the area of interest. Areas *A* and *B* have respective dimensions of 3.0 mm x 2.5 mm and 650 μm x 400 μm. A microscopic lens with a long working distance and a large zoom range (Optem Zoom 160) is used to enhance the magnification of observation.

4. Results and discussion

Fig. 4 shows the various steps of the proposed image processing method. A border line obtained by the Canny edge detection method together with a reference line are shown in Fig. 5. The height distribution of this line is calculated using the relationship between the projected light and that of the observation. The method works well on dark object but has the shortcoming of requiring a scanning device. The specimen is fixed on a stage drived by a step motor in the measurement system. As the stage is moved, the specimen surface is scanned by the projected optical edge, and a series of line profiles can be obtained. The measurement time for one specimen takes about 1 or 2 min depending on the dimension of the specimen. The final profile of the specimen is calculated by linear interpolation. Fig. 6(a) shows a continuous surface contour of the first specimen and Fig. 6(b) shows a corresponding 3D plot. The structures of the weaven fibers are clearly observed and the shape of fibers with valleys in between fibers is all clearly identified.

Normally, the shape of the valley in a black specimen is difficult to measure because of the low reflectivity and large unevenness on the surface. However, in this study, the structured light projected on the surface enabled the image to be separated into two distinct regions. In the dark region, little or no information is obtained. In the bright region, precise details in between fibers can be observed. It is to be noted that certain area

in the bright region, especially at the top of the weaven carbon fibers would have intensity above the dynamic range of the camera. This, however, will not significantly affect the results as only the intensity along the optical edge is of concerned.

To verify the proposed method, a phase shifting fringe projection method is also applied on the same specimen. Four phase shifted fringe patterns are captured as shown in Fig. 7(a). It is seen that the fringes are discontinuous and certain parts of the patterns are completely dark. Hence, it is not possible to record any useful information in this area. The wrapped and unwrapped phase maps are shown in Fig. 7(b) and (c), respectively. It is obvious from the phase maps that the profile of the specimen cannot be retrieved correctly.

To verify the capability of the proposed method for profiling a small object, a small test coin is used. A small area (Fig. 3(a) area *A*) is measured and the height distribution of area *A* calculated by the proposed method is shown in Fig. 8(a). The corresponding 3D plot is shown in Fig. 8(b). It is seen that the profile of area *A* is shown in precise detail with a very high resolution. A smaller area (Fig. 3(b) area B) with less than 100 μm in diameter (the eyeball of the animal) is also studied. It is seen that minute profile variation (Fig. 9) can be observed clearly. The height distribution of area B is shown in Fig. 10(a) and the corresponding 3D plot is shown in Fig. 10(b). It is seen that high quality surface profile with a resolution of 0.7 μm (the real size of one integral pixel) is obtained. The resolution of the technique is dependent on pixel size, it is possible to improve the resolution of the measurement by employing sub-pixels edge extraction approach [17,18].

It is noteworthy that the measurement of a small component requires a long working distance microscopic zoom lens with high magnification and the width of the projected optical edge should be narrow in order to minimize the introduction of errors due to an unfocused edge. In the present experiment, the width of the optical edge projected (w) is less than 10 pixels as shown in Fig. 9. As can be seen the edge contrast is not high. This is mainly due to the out-of-focus of the lens system and light diffraction on the projection edge. The effect of out-of-focus is similar to a convolution of a step function which describes the edge with a Gaussian distribution. The effect of light diffraction at the projection edge would result in a spread of the edge to that of a Sinc function on the object surface since the point spread function of a step function is a Sinc function. The out-of-focus and diffraction effect would result in the smoothening of the optical edge and hence could be utilized in the image processing instead of employing the convolution shown in Eq. (3). The effect of light diffraction is dependent on the optical setup and projection system and hence the diffraction effect is fixed. However, by adjusting the projection image lens, a slight out-of-focus effect on the optical edge can be achieved and the first processing step in the Canny's method can be implemented by optical method. Adjusting the out-of-focus within a suitable range will not introduce any errors while detecting the edges using the Canny's method.

It is worth noting that the resolution of the proposed method is lower than that of the phase shifting fringe projection method. In the proposed method, height information is

determined by comparing the distortion of a border line with a reference line. The minimal difference between the border line and the reference line is one integral pixel and hence a resolution of one pixel is achievable. It should be noted that the resolution is also dependent on the optical magnification of the observation system. In the first experiment, the actual size of one pixel which determines its resolution after calibration is 35 μm. In the second experiment, the corresponding resolution is 0.7 μm.

5. Concluding remarks

This paper presents a novel technique, an optical edge projection, to obtain the profile of a highly low-reflective object. Experiments have been carried out on a specimen fabricated by weaved carbon fibre material, where normal phase shifting fringe projection technique is not suitable. The proposed method can also be applied to 3D shape measurement on a small object with accuracy in the order of microns. The accuracy and resolution of the proposed method is determined by the recording sensor which is one pixel. The resolution, however, can be further improved with the introduction of a sub-pixel edge detection technique.

Acknowledgments

The authors acknowledge the financial supports provided by the National University of Singapore under Research Project R-265-000-140-112, and National Science Foundation of China (NSFC) under Contract Number 10302026.

References

[1] J.D. Hovanesian, Y.Y. Hung, Appl. Opt. 10 (1971) 2734.

[2] M. Idesawa, T. Yatagai, Appl. Opt. 16 (1977) 2152.

[3] C. Quan, P.J. Bryanston-Cross, Opt. Laser Tech. 22 (1990) 255.

[4] D.R. Burton, M.J. Lalor, Appl. Opt. 33 (1994) 2939.

[5] C. Quan, C.J. Tay, H.M. Shang, J. Mat. Proc. Tech. 89–90 (1999) 88.

[6] V. Sirnivasan, H.C. Liu, Appl. Opt. 23 (1984) 3105.

[7] X.Y. Su, W.S. Zhou, Opt. Commun. 94 (1992) 561.

[8] H.M. Shang, Y.Y. Hung, Opt. Eng. 139 (2000) 23.

[9] P.K. Rastogi, Opt. Laser Eng. 29 (1998) 103.

[10] C. Quan, X.Y. He, C.J. Tay, Opt. Commun. 189 (2001) 21.

[11] C. Quan, C.J. Tay, X.Y. He, Opt. Laser Tech. 34 (2002) 547.

[12] J.F. Canny, IEEE Trans. Pattern Anal. Machine Intell. 8 (1986) 679.

[13] H. Liu, K.C. Jezek, Int. J. Remote Sensing 25 (2004) 937.

[14] K. Creath, Prog. Opt. 26 (1998) 349.

[15] D.C. Ghiglia, L.A. Romero, J. Opt. Soc. Am. A 11 (1994) 107.

[16] M. Takeda, H. Ina, S. Kobayashi, J. Opt. Soc. Am. 72 (1) (1982) 156.

[17] Y. Shan, G.W. Boon, Image Vision Comput. 18 (2000) 1015.

[18] K. Jenson, D. Anastassiou, IEEE Tran. Image Proc. 4 (3) (1995) 285.

List of Figures

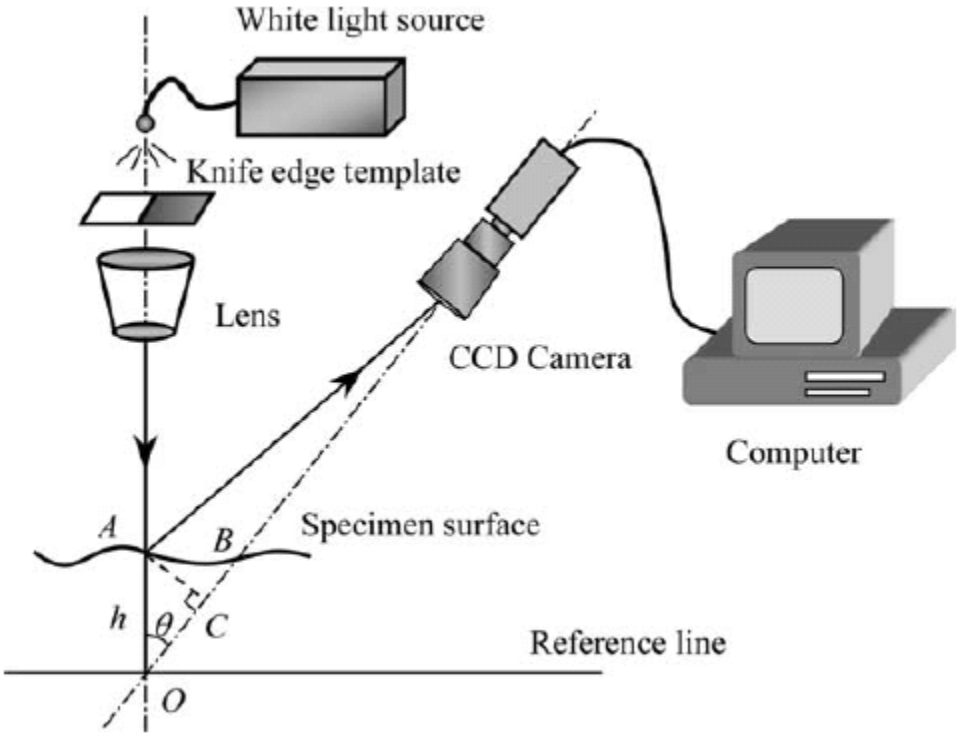
White light source
Knife edge template
Lens
CCD Camera
Computer
A
B
Specimen surface
h
θ
C
Reference line
O

Fig. 1

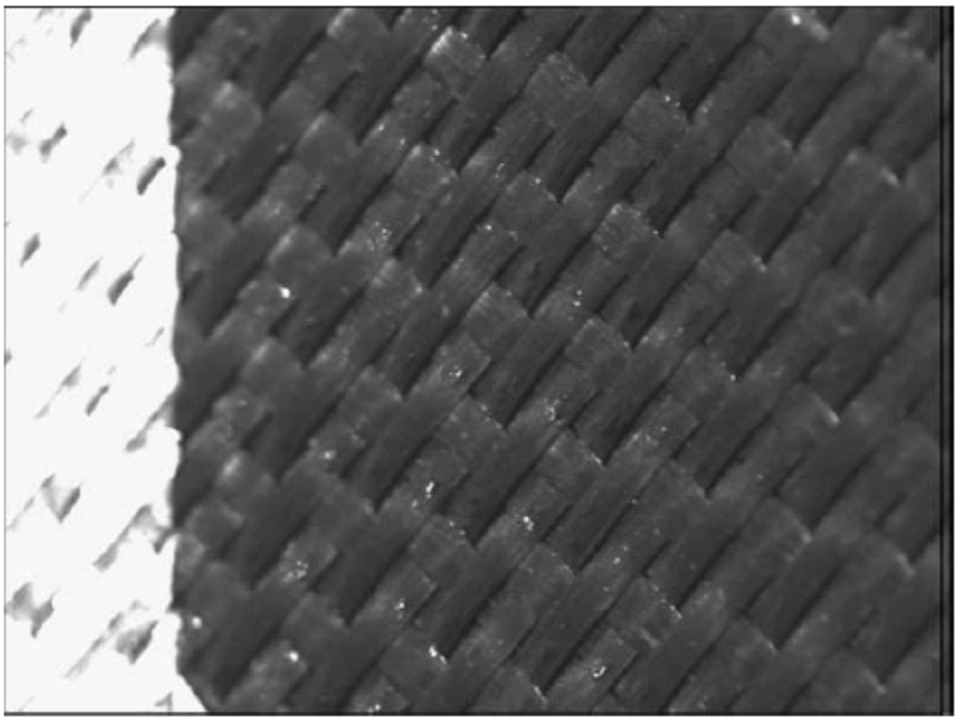

Fig. 2

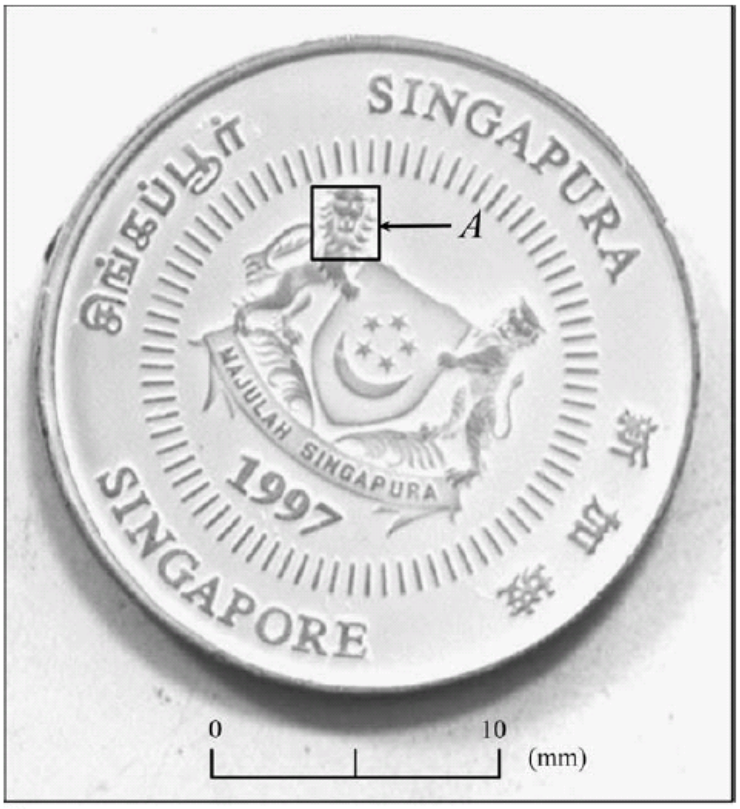
SINGAPURA
சிங்கப்பூர்
新加坡
SINGAPORE
1997
MAJULAH SINGAPURA
A
0
10
(mm)

a

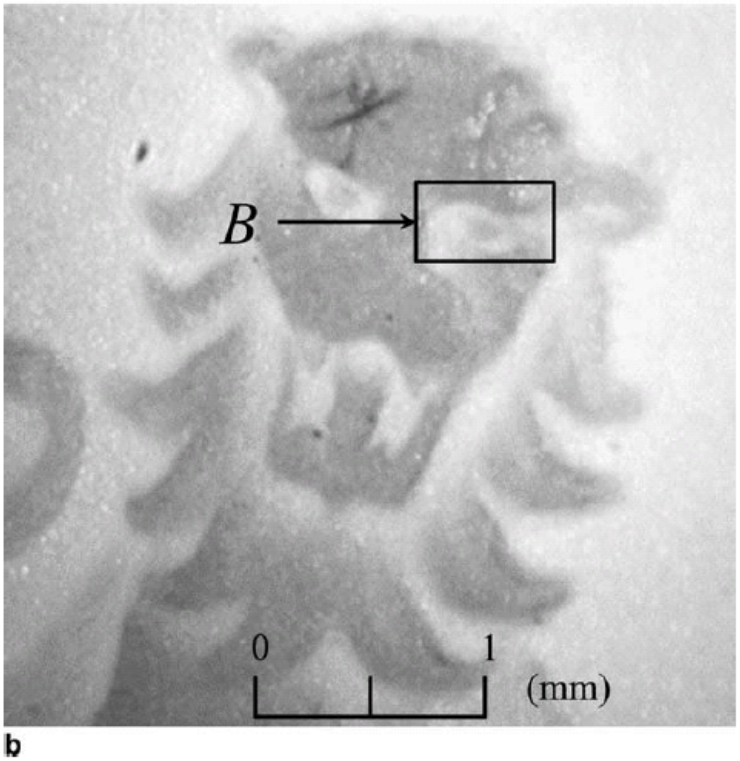
B
0
1
(mm)

b

Fig. 3

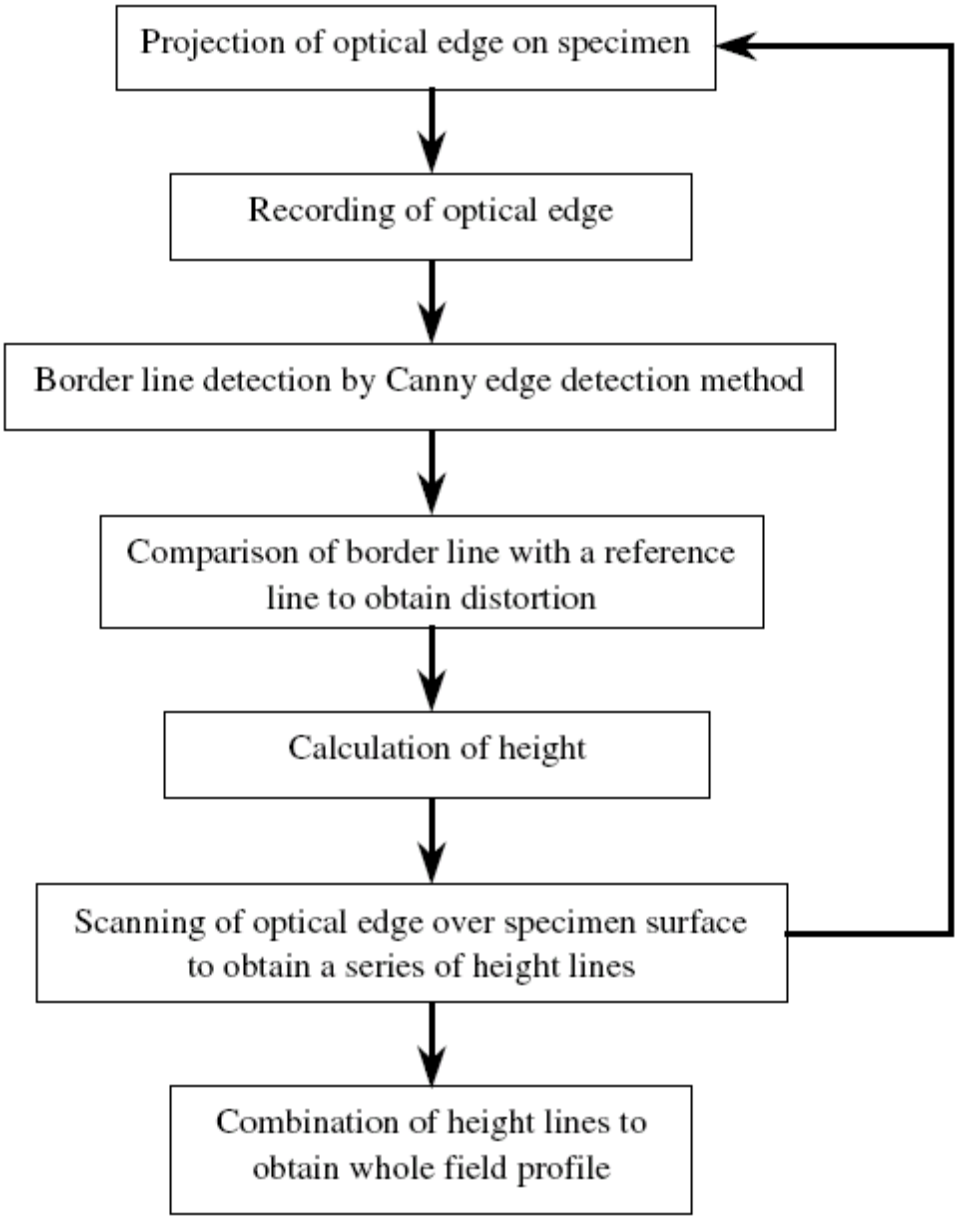
Projection of optical edge on specimen
Recording of optical edge
Border line detection by Canny edge detection method
Comparison of border line with a reference line to obtain distortion
Calculation of height
Scanning of optical edge over specimen surface to obtain a series of height lines
Combination of height lines to obtain whole field profile

Fig. 4

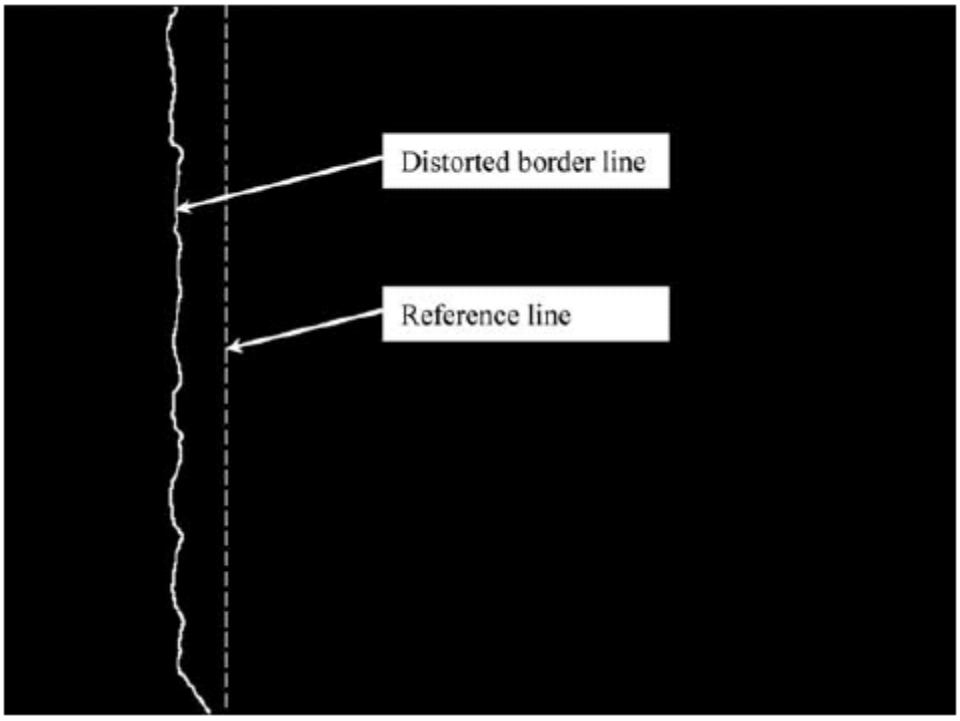

Fig. 5

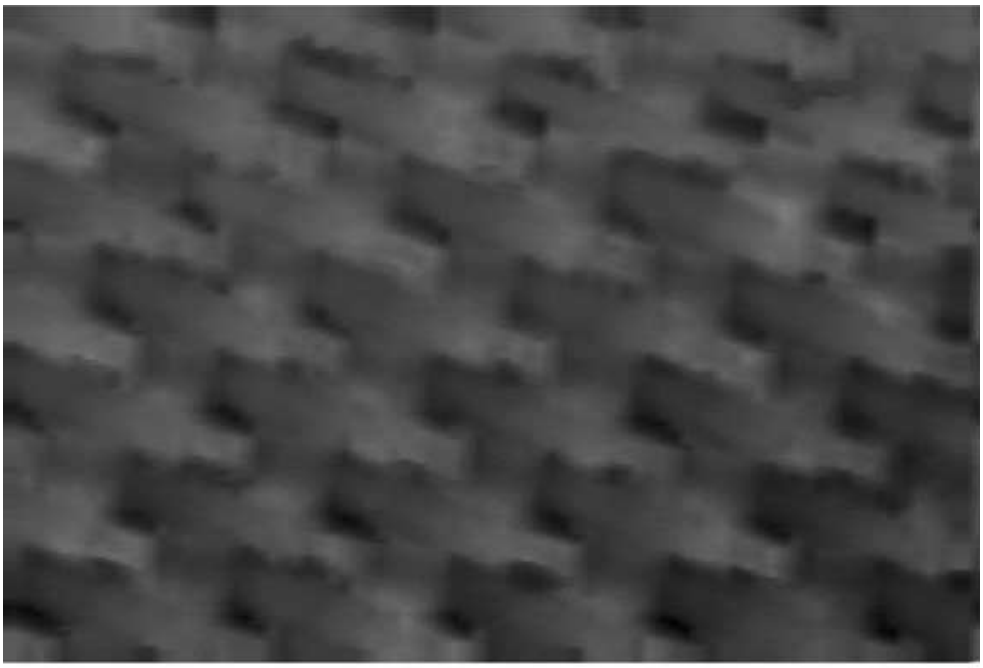

a

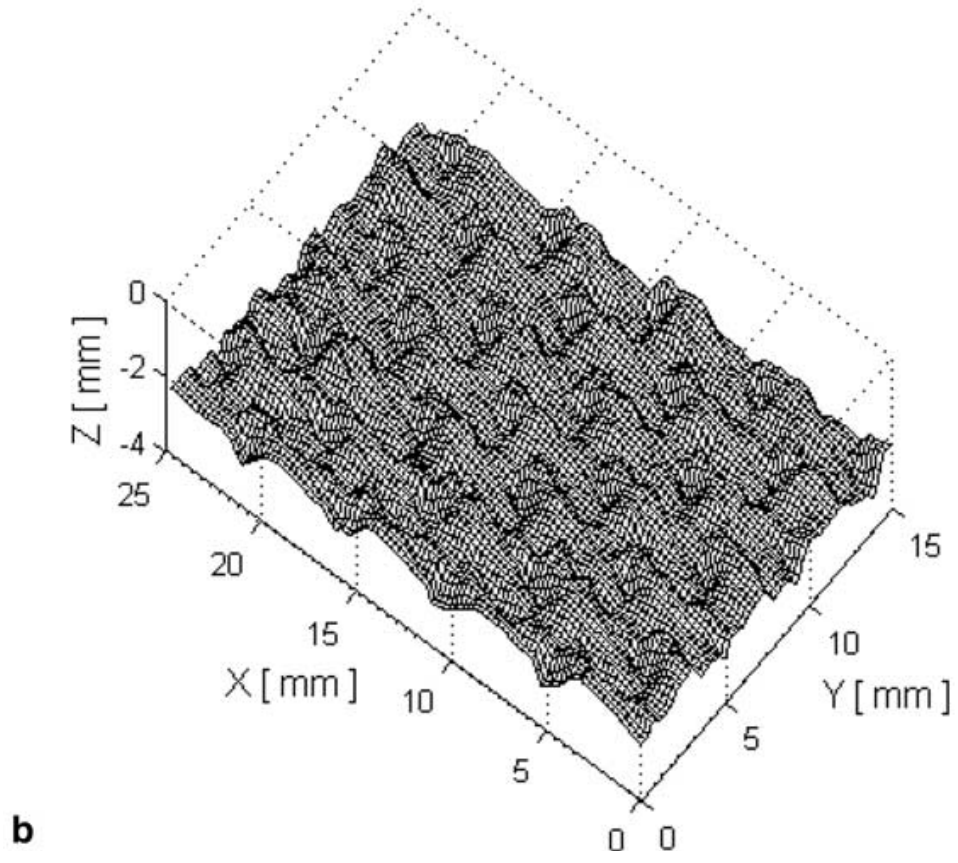

b

Fig. 6

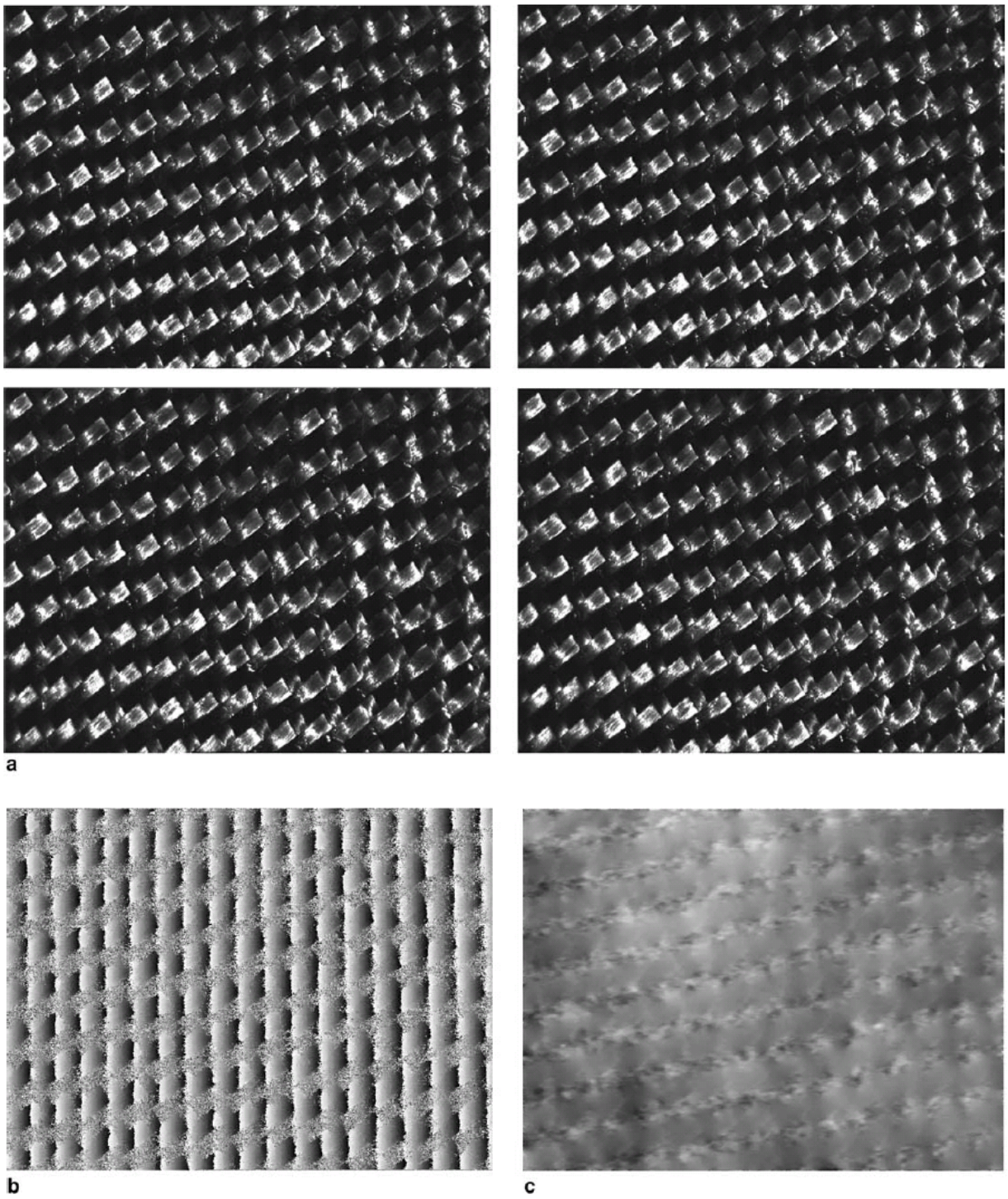

Fig. 7

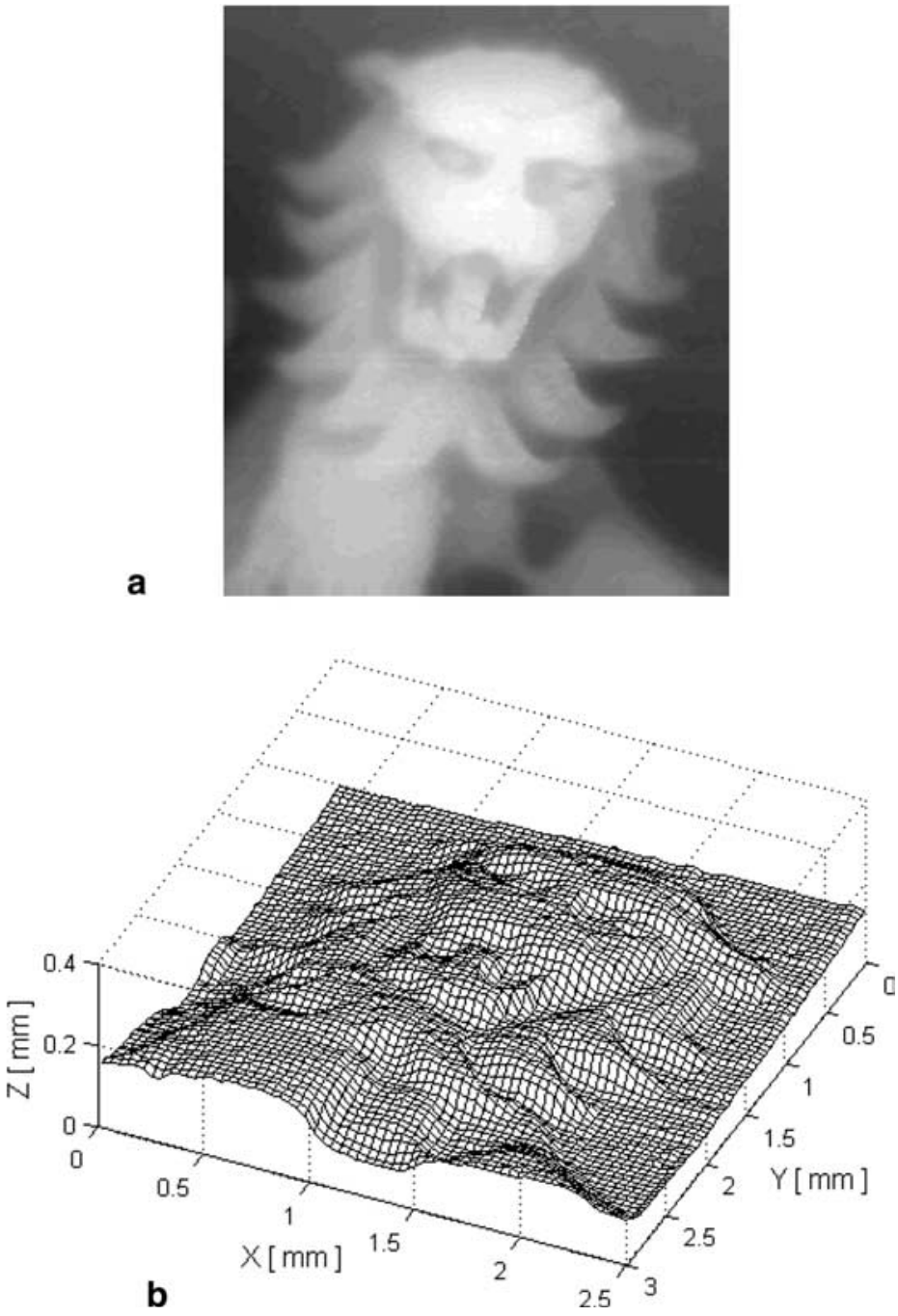

Fig. 8

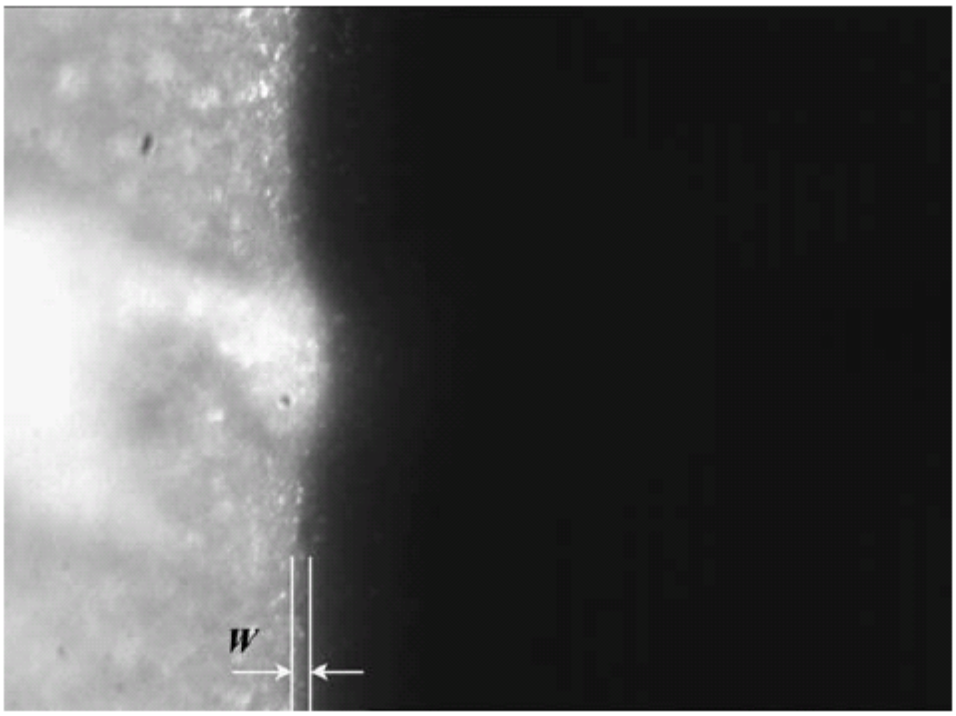

Fig. 9

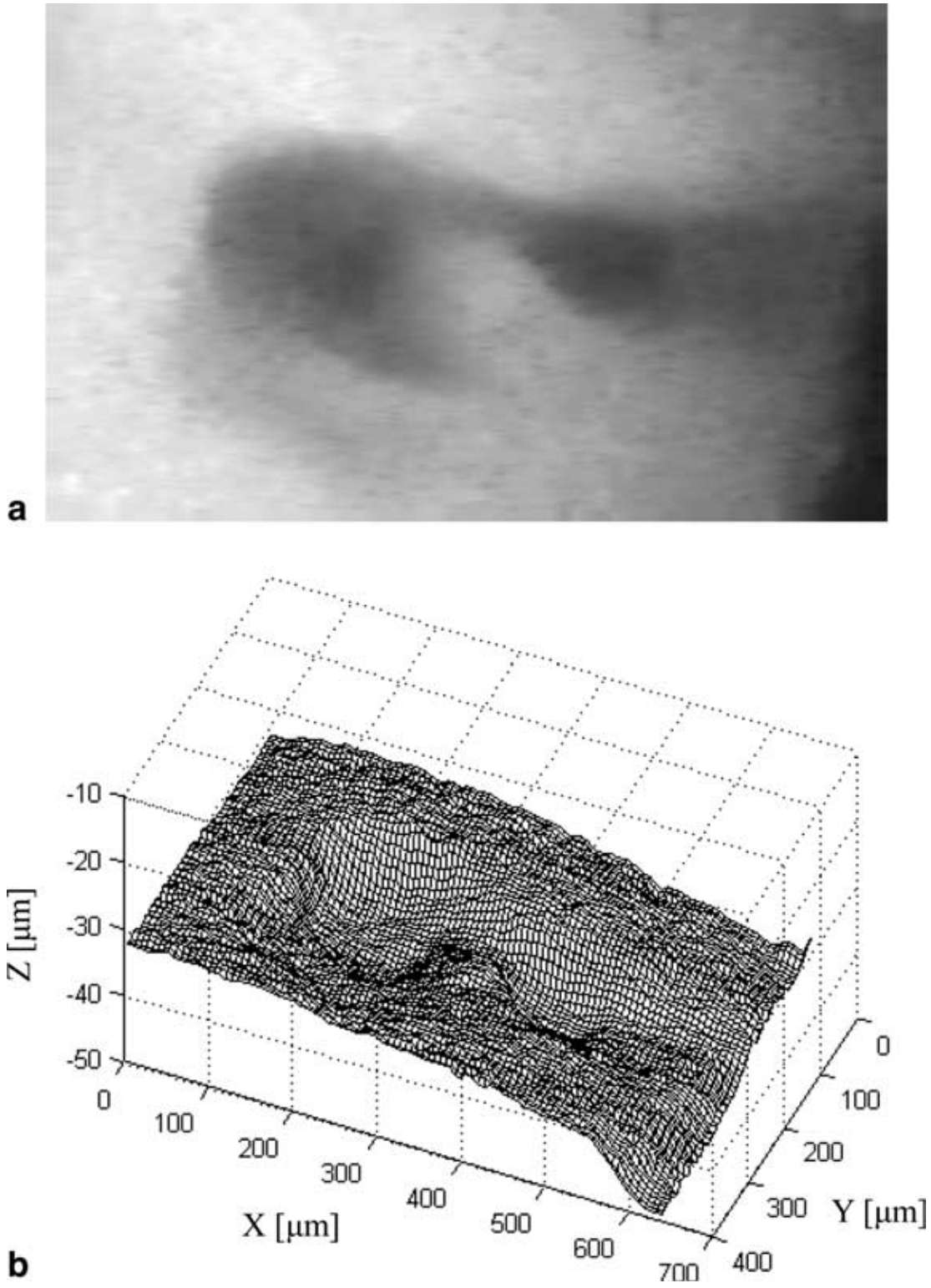
a
b
Z [µm]
-10
-20
-30
-40
-50
0
100
200
300
400
500
600
700
X [µm]
0
100
200
300
400
Y [µm]

Fig. 10